33RD INTERNATIONAL COSMIC RAY CONFERENCE, RIO DE JANEIRO 2013
THE ASTROPARTICLE PHYSICS CONFERENCE

ICRC 2013

Measurement of the Optical Properties of the Auger Fluorescence Telescopes

JULIA BÄUML[1] FOR THE PIERRE AUGER COLLABORATION[2]

[1] *Karlsruhe Institute of Technology, Karlsruhe, Germany*
[2] *Full author list: http://www.auger.org/archive/authors_2013_05.html*

auger_spokespersons@fnal.gov

Abstract: Fluorescence telescopes are used for the calorimetric measurement of the energy of air showers at the Pierre Auger Observatory. The optical properties of these telescopes have to be known precisely to allow for an absolute energy calibration. We present a method to measure their light distribution function independent of shower data. We have developed an isotropic, point-like light source, that was brought into the field of view of a telescope using an autonomously flying platform, an octocopter. The optical properties of the telescopes are probed in detail by illuminating the telescopes from different angles with respect to the telescope axis and by obscuring or removing certain telescope components. In this contribution, we describe the light source which was developed and the important properties of the octocopter. We further present the first results on the measured light distribution and compare them to detailed telescope simulations.

Keywords: Pierre Auger Observatory, fluorescence telescopes, optical properties, point spread function, calibration, light source, octocopter

1 Introduction

The Pierre Auger Observatory is a hybrid detector allowing for the measurement of air showers with an array of water-Cherenkov detectors and fluorescence telescopes [1]. The number of fluorescence photons produced by an air shower in the atmosphere is proportional to the energy deposited by the shower. Therefore, the observed fluorescence light profile can be used to obtain an estimate of the calorimetric energy of an air shower and hence the energy of the primary particle. The shower energy derived this way is almost independent of shower simulations and, in particular, hadronic interaction models. A set of showers observed simultaneously with the surface detector array and the fluorescence telescopes on clear dark nights (14% of the overall measurement time) is used to derive an energy calibration for the surface detector, which reaches a duty cycle of $\sim 100\%$.

The fluorescence telescopes [2] are calibrated with an end-to-end method using a drum that covers and uniformly illuminates the entire telescope aperture [3]. An air shower, on the other hand, is equivalent to a localized, almost point-like light source. To analyse the shower profile it is necessary to reconstruct the light distribution at the aperture, accounting not only for the transfer function measured with the drum calibration, but also for the point spread function of the telescope.

In this paper we discuss a novel technique to study the optical properties of fluorescence and atmospheric Cherenkov telescopes and present a first measurement of the point spread function of the Auger telescopes. The same method can be used to measure the telescope pointing or to obtain an absolute calibration of individual pixels of fluorescence telescopes, see [4].

A portable, point-like light source is placed in the field of view of a telescope by an octocopter. The GPS- and pressure-sensor-based positioning system of the octocopter can be programmed to place the light source at different distances and altitudes for a duration of up to 20 min. The light source has an isotropic emission pattern and the intensity of the flashes of UV light is electronically stabilized. The camera of the fluorescence telescope is read out for each flash, including non-triggered pixels. Averaging over many images taken for the same position of the light source gives access to the tail in the point spread function that is otherwise dominated by the noise of the background light.

After describing the custom-built light source and its calibration in laboratory measurements we will briefly summarize the parameters of the commercially available octocopter in Sec. 2. Using this setup an extensive set of measurement campaigns has been carried out and point spread functions for different telescopes have been derived. First results will be presented in Sec. 4 and compared to simulations of the optical properties of the telescopes. Implications for the fraction of light of a shower image within a few degrees of the shower axis as well as the interpretation of the telescope calibration will be discussed in Sec. 5.

2 Experimental setup

2.1 The light source

Our requirements for the light source were threefold: isotropy, light weight and emittance in the UV range. As light emitters we use LEDs of type H2A1-H375 from Roithner Laser [5]. Their spectrum has its peak at 375 nm and lies within the range of high telescope efficiency (see Fig. 1).

To achieve the best possible homogeneity, a total of 12 LEDs were distributed evenly on a sphere. The centres of the faces of a dodecahedron provide such a distribution. To improve the homogeneity of the light distribution, the body of the light source with mounted LEDs was coated with Tyvek and surrounded by a diffuser bowl. As diffuser we use a clear polystyrene sphere made up of two hemispheres, which we etched with acetone to make them diffuse. To reduce the weight of the light source and to make it as compact as possible, the LEDs were detached from their hexagonal mounting plates. Based on simulations of the

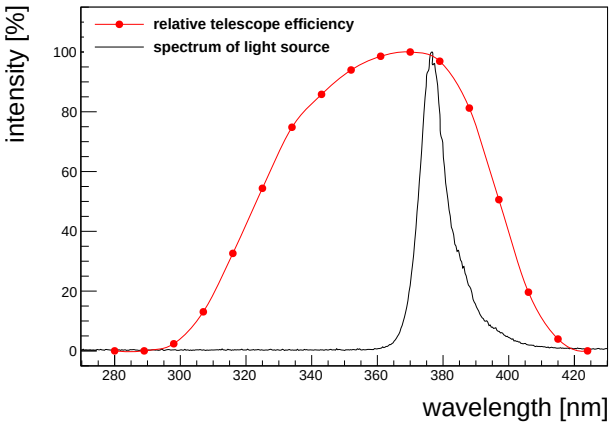

Figure 1: Spectrum and telescope efficiency. The spectrum of the LEDs being used lies within the range of high telescope efficiency. The measured spectra of a single LED and the complete light source agree well, there is no spectral effect of the surrounding diffuser bowl.

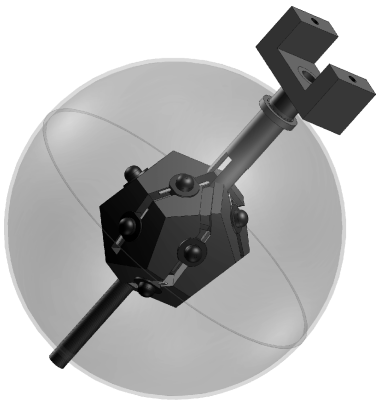

Figure 2: Schematic drawing of the light source. The LEDs are mounted on a dodecahedron-shaped body made from ABS. Channels for all cabling are embedded in the body as well as the supporting rod. The diffuser bowl surrounding the dodecahedron is fixed to the supporting rod, which also attaches the light source to the octocopter.

resulting light distribution with a diffuser sphere of radius 50 mm, the edge length of the dodecahedron was chosen as 16 mm. The body was printed with a 3D printer from Acrylonitrile Butadiene Styrene (ABS) based on a 3D model of the dodecahedron with embedded sockets for the LEDs and channels for all cables (see Fig. 2).

The homogeneity that was achieved with this setup is very good. The maximum difference in intensity between the hottest and the coldest spot over a range of $\pm 18^\circ$ is 3.5%. The actual pointing direction of the light source towards the telescope is monitored during measurement campaigns, which allows for a correction of the intensity differences.

The electronic board driving the LEDs has twelve output channels. Emitted light pulses can have durations between 2 μs and 64 μs and one of six adjustable amplitudes. They are triggered by the PPS signal of the on-board GPS receiver with a programmable delay between 50 μs and 1000 μs. For other purposes a DC operation is also possible. All properties can be configured via an I^2C interface.

For monitoring, a photodiode and a temperature sensor

Figure 3: Octocopter with light source. The eight engines of the octocopter are arranged on a circle. Their supporting rods are connected to a central platform carrying all circuit boards for operation and communication. The light source is attached to the supporting rods of the two engines that define the forward direction.

are placed inside the diffuser bowl, a second temperature sensor is attached to the electronics board.

The energy emitted by the light source has been measured using a NIST-calibrated photodiode and an electrometer (charge measurement). The accuracy that can be reached in those measurements is as good as $\sim 2\%$. During measurement campaigns at the Telescope Array [6], intensity measurements were made at the University of Utah. Those measurements, with an independent setup using a different NIST-calibrated photodiode and a picoammeter (current measurement), have confirmed the intensity and accuracy values [4].

The value for the absolute intensity of the light source depends slightly on the rate of the emitted light pulses (for feasibility reasons 1 kHz in the lab, 1 Hz in telescope measurements) and the temperature. Furthermore the length of the pulse changes slightly with the amplitude. All of those effects have been studied in great detail and can be corrected for to achieve an absolute calibration.

2.2 The octocopter

We employ a flying platform to bring the light source into the field of view of a telescope. The octocopter, a Mikrokopter [7, 8] with eight motors, was chosen for reliability reasons. A failure of any two motors does not affect its self-stabilization capabilities. When given a set of GPS coordinates, timing and pointing directions, the octocopter performs an autonomous way-point flight in 3D, controlled by GPS and a magnetic field sensor. The octocopter is able to keep its position and pointing within ~ 1 m (+ GPS uncertainty) and $\sim 5^\circ$, respectively, in moderate wind conditions. Payload weights of up to 1 kg can be lifted and flight times of up to 20 min can be achieved with the light source attached. Due to the open platform, it was possible to integrate the hardware and software of the light source closely into the existing octocopter system.

2.3 Measurement campaigns

Measurements with the octocopter and light source device can only take place during the regular data taking periods of the fluorescence detector (moonless nights, no rain)

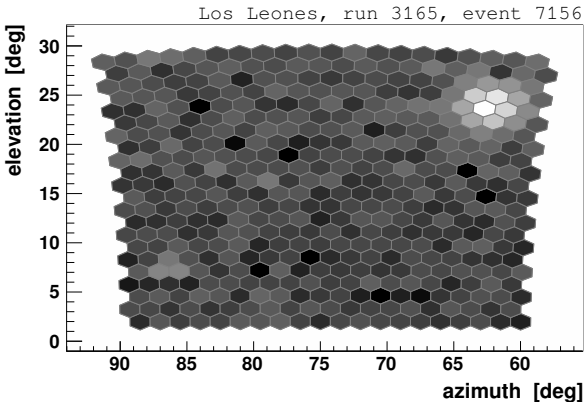

Figure 4: Example of a measured flasher event. The hexagons denote the pixels of the FD camera and the main spot is clearly visible in the upper right corner. The logarithmic signal in each pixel is indicated by grey-scale colours.

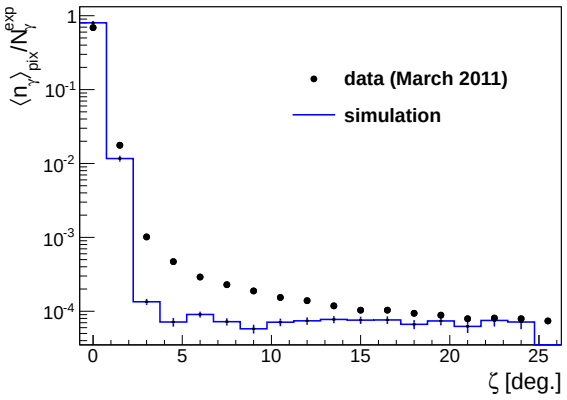

Figure 5: Differential light distribution from data (dots) and simulation (histogram). Shown is the average number of photons detected per pixel, $\langle n_\gamma \rangle_{\mathrm{pix}}$, normalised to the expected total number of photons on the aperture, N_γ^{exp}.

when the wind speed is no higher than 5 m/s. We use an external trigger set to the time of the light pulse, so that the normal data taking is not interrupted, just the dead-time of the telescope is increased. The external trigger mode further allows us to read out all pixels in the triggered telescope. The octocopter is usually flown at distances of $0.5 - 1$ km to the telescope. At such distances, the GPS position uncertainty of ± 6 m is smaller than the angular size of one telescope pixel (1.5° corresponds to 13 m at 500 m or 26 m at 1 km).

GPS way-points and the duration per position are programmed into the octocopter to probe the desired pixels in a telescope. The number of light source pulses per way-point is fixed by the pulse frequency of 1 Hz. Over the past few years, campaigns with different setups have been carried out. Several pixels with different positions on the telescope camera have been probed. The position of the light spot on the surface of a pixel has also been varied, changing from a position well centred on a PMT to positions right on top of a light collector between two pixels. For comparison, measurements have been made for several different telescopes and using varying distances between telescope and light source. To study the optics of the telescope in more detail, telescope components like the mirror, the camera, the corrector lens or the filter have been manipulated (e.g. cleaned), covered or removed. An example of a measured flasher event is shown in Fig. 4.

3 Simulations

To simulate the response of the telescope to the flasher light source, we use the Auger Offline Framework [9]. It offers two modules for the simulation of the telescope. The standard module is based on simple ray tracing and enables very fast telescope simulations. The ray tracing has been enhanced step by step with more and more knowledge of the telescope optics. Single telescope components can be modified, included or excluded from the photon path, allowing for easy comparison with data taken during octocopter campaigns. The results obtained with the improved ray tracing are confirmed with the second module for telescope simulation that is based on GEANT4 [10]. It allows for a very precise simulation, but due to its precision, its computational requirements are too large to allow usage for standard shower simulations.

4 Point spread function

The optical spot diameter of the Auger fluorescence detector is about 0.5° [2]. During measurements it was found that photons from the light source are detected not only in the directly hit pixels but also in most other pixels of the camera. This spread of light, the *halo*, has been subject to research and can partially be explained by detailed simulations of the telescope optics. The measured and simulated angular distributions of light are shown in Fig. 5. They have been obtained by averaging over many events recorded during one octocopter flight in front of telescope 3 at the Los Leones site. For all events the position of the light source, i.e. the centre of the light spot, is assigned to $\zeta = 0°$. The mean value of the signals detected in all pixels with a certain angular distance to the spot centre is plotted versus the corresponding angles. We observe a broadened spot at small angles due to the convolution of the pixel size of 1.5° and the finite spot size of 0.5°. The observed width of the smeared peak depends on the distribution of spot positions on the pixel in the shown data set. With increasing distance to the spot centre the observed signal decreases further and forms a more or less flat tail. The signal however does not decrease as steeply as expected from simulations when going out from the spot centre and about 15% of the light is spread to angles larger than 2°. A second spot, a ghost image point symmetric to the centre of the camera, is observed as well (see Fig. 4). Since its angular distance to the spot centre depends on the position of the spot on the camera, the ghost region has been excluded in the estimation of the point spread function shown.

The point spread function changes only very little for different positions of the spot on the camera and for different distances between the light source and the telescope. Measurements with several telescopes at different fluorescence detector sites show very small changes in the light distribution. A clear difference can be seen between an event sample where the light spot is well within one pixel and another sample where the spot is centred on top of a light collector between two pixels.

The main part of the halo is caused by reflections inside

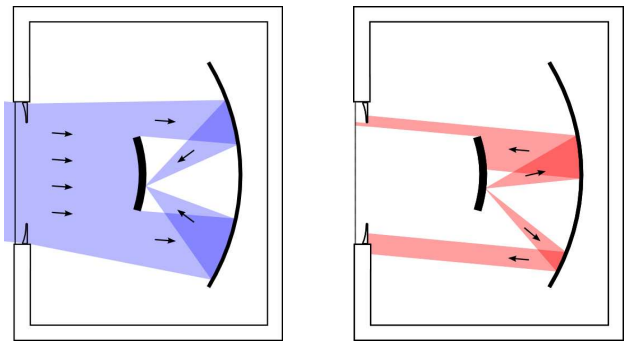

Figure 6: Telescope schematics and illustration of PMT reflections. Parallel light entering the telescope from the left hand side traverses the UV-filter at the aperture and the annular corrector lens before it is focused onto the camera (left). Part of the light is reflected on the surface of the camera and is consequently reflected back in the direction of the camera and the aperture by the mirror. This results in a very wide illumination of the camera (right). The part of the light that reaches the aperture of the telescope again can be reflected back to the mirror and is then focused onto a second spot point symmetrically placed about the centre of the camera.

the telescope bay. Most of the large tail of the distribution at angles above $\sim 15^\circ$ is caused by light that has been reflected off the surface of one of the pixel PMTs of the camera (see Fig. 6). The reflectivity of the PMTs has been measured in lab experiments and was found to be about 20%, depending on the position on the PMT, the incidence angle and the wavelength. Parts of the light reflected at the PMT surface, for reasons of symmetry, hit the camera in a broad beam, illuminating a large number of pixels. Due to the camera shadow in the incoming light beam, the actual illumination of the camera depends on the position of the spot. The distributions however resemble each other when viewed with respect to the spot centre. If the spot lies well on top of one of the light collectors surrounding all pixels, the back reflections are different. This is clearly visible in the resulting light distribution.

The back-reflected light that does not hit the camera can be reflected again at the aperture of the telescope and is consequently focused in the ghost spot. The intensity of this ghost spot is about 0.4% of the main spot.

Part of the widening of the spot is caused by multiple reflections inside the telescope bay, mainly reflections between the corrector lens and the UV-filter that forms the aperture window. Those reflections disturb the incoming direction of the photon and cause it to be detected in one of the pixels neighbouring the one containing the main spot.

These effects that cause the broadening of the light distribution have been included into the telescope simulations (see Fig. 5). The point spread function derived from simulations describes the measured one well at small angles below $\sim 2^\circ$ and at large angles above $\sim 15^\circ$ to the spot centre. In the intermediate range, some signal is also produced in simulations, although not enough to describe the data.

5 Discussion

The measured point spread function is of relevance to shower measurements in two ways: (i) During a drum calibration, all pixels in a camera are simultaneously illuminated. The interpretation of the signals recorded in each pixel therefore directly depends on the point spread function of the optics. (ii) For shower reconstruction, light within an angular region of $\zeta_{\rm opt}$ is considered. The size of $\zeta_{\rm opt}$ is determined by the optimal signal to noise ratio. The point spread function of the telescope reduces the fraction of light inside a circle with opening angle $\zeta_{\rm opt}$.

Despite various cross-checks and measurements of the influence of individual optical components of the telescope on the point spread function, part of the light distribution is still not fully understood, i.e. cannot be reproduced in simulations. This amounts to about $5-6\%$ of the direct light. Multiple scattering in the atmosphere is very unlikely to be a major source: measurements at different distances between the light source and telescopes show no distance dependence. The effect of different aerosol sizes on the light distribution is under investigation. First measurements with a similar light source have been made in 2008. Since then, no significant change in the point spread function has been observed. Current studies focus on measuring individual telescope components in the lab and testing for possible effects of ageing.

Our current understanding of the point spread function requires a change of the drum calibration constants by $3-4\%$. This correction factor has been estimated using simulations and verified by direct measurements inside the telescope bay. Updated calibration constants accounting for this effect are now used for analyses of data from the fluorescence detector. The impact of the measured point spread function on the energy scale of the Pierre Auger Observatory is addressed in detail in [11].

The calibrated point-like light source can also be used to calibrate the fluorescence detector. In contrast to the standard calibration procedure using the drum, the new method results in calibration constants for single pixels within a camera. The calibration of a full camera would be very time consuming and probably not feasible. It provides, however, a systematically independent measurement that can be used to test the current calibration procedure. This method is currently being applied for cross-calibration of the fluorescence telescopes of the Pierre Auger Observatory and the Telescope Array [4].

References

[1] The Pierre Auger Collaboration, Nucl. Instrum. Meth. A **523** (2004) 50
[2] The Pierre Auger Collaboration, Nucl. Instrum. Meth. A **620** (2010) 227
[3] J.T. Brack et al., Astropart. Phys. **20** (2004) 653; JINST **8** (2013) P05014
[4] J.N. Matthews et al., for the Telescope Array and Pierre Auger Collaborations, paper 1218, these proceedings
[5] Roithner Lasertechnik GmbH, http://www.roithner-laser.com
[6] K. Machida, for the Telescope Array Collaboration, paper 0504, these proceedings
[7] Mikrokopter website, http://www.mikrokopter.de
[8] HiSystems GmbH, https://mikrocontroller.com
[9] J. Allen et al., J. Phys. Conf. Ser. **119** (2008) 032002
[10] The GEANT4 Collaboration, Nucl. Instrum. Meth. A **506** (2003) 250
[11] V. Verzi, for the Pierre Auger Collaboration, paper 0928, these proceedings